Spin dependent electronic band structure of Co/Cu(001) with different film thicknesses

K. Miyamoto[a] * , K. Iori[a], K. Sakamoto[a], A. Kimura[a], S. Qiao[b], K. Shimada[b], H. Namatame[b] and M. Taniguchi[a,b]

[a]Graduate School of Science, Hiroshima University, 1-3-1 Kagamiyama, Higashi-Hiroshima 739-8526, Japan

[b]Hiroshima Synchrotron Radiation Center, Hiroshima University, 2-313 Kagamiyama, Higashi-Hiroshima 739-0046, Japan

E-mail: kmiyamoto@hiroshima-u.ac.jp

Abstract.

Spin- and angle- resolved photoemission spectroscopy has been applied to the study on spin polarized electronic structures of fct Co thin film with thicknesses from 2 ML to 9.5 ML. We have clearly observed two dispersive majority and minority spin band structures originating from the bulk-like bands. These observed band structures show narrower width for thinner film due to an in-plane lattice expansion at the Co-Cu interface.

PACS numbers: 75.70.Rf, 79.60.-i

* To K. Miyamoto (kmiyamoto@hiroshima-u.ac.jp)

1. Introduction

The magnetic thin films are expected to show peculiar magnetic properties such as an enhanced magnetic moment, a strong magnetic anisotropy and a reduced Curie temperature, which are generally much different from those of bulk [1-3]. The metallic synthetic lattice, which is a nano-scale magnetic material grown on a semiconductor or a metallic surface, has lately attracted a considerable attention. In metallic thin film, the difference in the lattice constant of substrate results in variation of structure and magnetic properties. It is known that bulk Co has a hexagonal close-packed (hcp) structure at room temperature. In contrast, Co growing in the fcc lattice shows a small tetragonal distortion (~ 4 %) along the surface normal [4]. As for magnetic properties, Co/Cu(001) shows an in-plane magnetic anisotropy along [1$\bar{1}$0] direction and a Curie temperature exceeds room temperature already at 2 ML [5]. Enhanced spin and orbital magnetic moments for thinner films of Co/Cu(001) have been experimentally clarified by x-ray magnetic circular dichroism technique [6]. Such an enhancement could be pertinent to a reduced dimensionality, which might cause a large exchange splitting and/or a strong electron localization. The enhancement of $3d$ exchange splitting was suggested for 2.4 ML Co/Cu(001) by spin resolved PES at $\bar{\Gamma}$, where the energy dispersion feature was missing [7]. Co/Cu superlattice is well known to show an oscillatory magnetic interlayer coupling [8] as well as a giant magneto-resistance (GMR) at room temperature [9]. Such striking magnetic and transport propeties are determined by spin-dependent electronic structure at the Co-Cu interface. It is expected that the knowledge of momentum- and spin-dependent electronic structures of face-centered tetragonal (fct) Co/Cu(001) in the vicinity of the Fermi level ($E_{\rm F}$) would help us to understand the behaivor of spin polarized electron current in multilayer systems. Motivated by these aspects, we have tried to clarify how the Co $3d$ states depend on the film thickness ($>$ 2ML) by spin- and angle- resolved photoelectron spectroscopy (SARPES) in the wide range of Brillouin zone.

2. Experimental

A clean surface of Cu substrate was obtained by repeated cycles of Ar-ion bombardment (1-2 keV) and annealing at 720 K in an ultra high vacuum condition. Co thin film was epitaxially grown by a commercial evaporator at the deposition rate of $0.1 \sim 0.2$ ML/min in a pressure of 5×10^{-8} Pa. The substrate was kept at room temperature during the Co film growth. The cleanliness and flatness of the substrate and film surfaces were checked by means of Auger electron spectroscopy (AES) and reflection high energy electron diffraction (RHEED). The Co film thickness was estimated from RHEED as well as the intensity ratio of the Co 1st LMM signal ($E_k = 670$ eV) to that of the Cu 3rd LMM ($E_k = 940$ eV) in the AES spectrum. The spin- and angle- resolved photoelectron spectroscopy (SARPES) was performed using our home-made system equipped with a 125 mm radius hemispherical electron analyzer (Omicron: EA-125) and the retarding

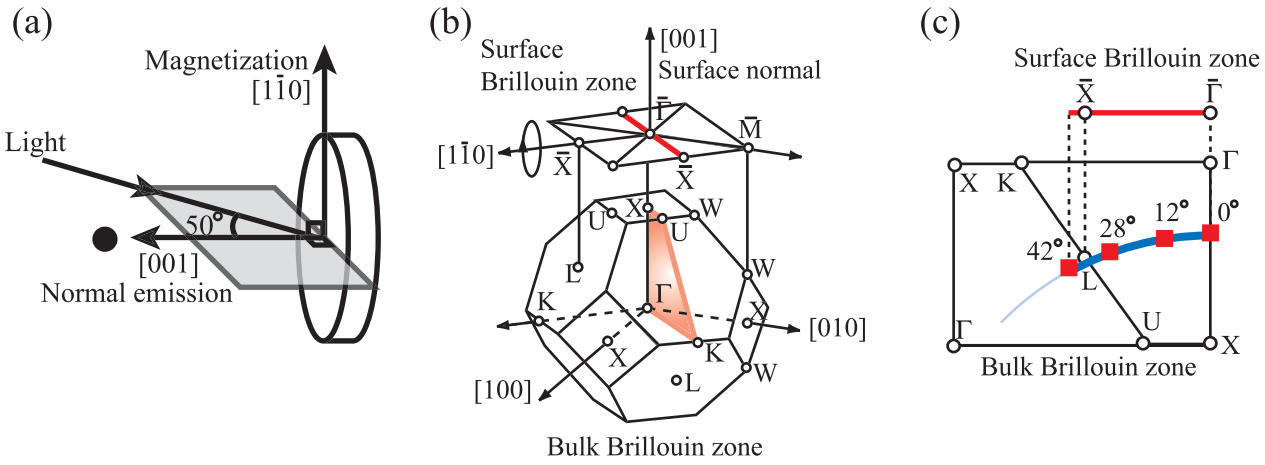

Figure 1. (a) Experimental setup for SARPES measurements of fct Co/Cu(001). (b) Surface and bulk Brillouin zones for (001) surface of fcc lattice. Here, thick line along $\bar{\Gamma}$-$\bar{X}$ in surface Brillouin zone and shaded area in bulk Brillouin zone show observed direction and area in the present experiment. (c) Cross section of the bulk Brillouin zone at ΓXUK plane. Thick line and square symbol corresponds to the measured wave numbers at $E_{\rm F}$ in this experiment.

type Mott spin polarimeter in Hiroshima Synchrotron Radiation Center, which was originally designed by Qiao et al. [10]. Moreover, we have evaluated the efficiency of the spin polarimeter such as effective Sherman function and the intensity of scattered electrons with our recently developed self-calibration method [11]. All of the spectra were measured at room temperature (T $\sim$ 300 K) and excited by unpolarized He I_α resonance line ($h\nu \sim 21.2$ eV). Angular acceptance of photoelectron was set to 2° at a pass energy of 5 eV. The energy resolution is 110 meV with these experimental conditions as checked by the spectrum of polycrystalline gold close to $E_{\rm F}$. The geometry of the measurement is shown in Fig.1 (a). The sample was magnetized along in-plane [1$\bar{1}$0] direction by a coil wound around a $\mu-$metal yoke. The measured spin component for the present experiment is aligned along the magnetization direction. The angle of incident light was 50° relative to surface normal. In Fig.1 (b), thick line represents $\bar{\Gamma}-\bar{X}$ line in the surface Brilloin zone and shaded area denotes ΓXUK plane in the bulk Brilloin zone, which are traced in the present experiment. A free electron final state assumes the parallel and perpendicular wave-number components of electronic state at $E_{\rm F}$ as $k_{//} = 0.512\sqrt{h\nu - E_{\rm B} - \phi}\cdot\sin\theta$ and $k_{\perp} = 0.512\sqrt{(h\nu - E_{\rm B} - \phi)\cos^2\theta + V_0}$, respectively, as denoted by thick curve in Fig.1 (c), where $h\nu$, $E_{\rm B}$, ϕ and V_0 represent photon energy, binding energy, work function and inner potential. Here, the inner potential V_0 of 15 eV has been referred to the previous report [13]. The spectra were recorded by repeated scans and the direction of magnetization was reversed for every new scan to cancel out the instrumental asymmetry. The magnetization reversal also minimizes a contribution of spin-orbit induced spin polarization compared to that induced by the exchange-interaction, which are of the interest in this work [13, 14].

3. Results and Discussion

Figures 2 (a) and (b) show the SARPE spectra and the spin polarizations of 9.5 ML Co/Cu (001) at the emission angles (θ) of 0° - 42°. Here, majority and minority spin spectra are shown with open and filled triangles, respectively. Thick (thin) vertical bars show the peak positions of Co 3d states in the majority (minority) spin channel. At θ = 0°, the minority spin spectrum possesses a peak at the binding energy (E_B) of 0.21 ($\pm$0.09) eV as denoted by A in Fig.2 (a). The peak A shifts toward higher $E_{\rm B}$ with increasing θ and reaches $E_{\rm B}$ maximum around θ = 37° ($\bar{X}$ point). In contrast, a broad peak (named as B) is found for the majority spin spectrum at $E_{\rm B}$ = 0.8 ($\pm$0.12) eV, showing energy shift toward lower E_B with increasing θ and it reaches near $E_{\rm F}$ at θ = 12°. In the normal emission spectrum, the observed features of majority and minority spin spectra are in principle consistent with the reported result with a different photon energy of $h\nu$ = 24 eV [12]. Here, we have found the largest negative spin polarization of -50 % near $E_{\rm F}$ and a positive value of 30 % in the $E_{\rm B}$ region of 1.5-2.0 eV without exhibiting any distinct structures. The minimum of negative spin polarization moves to higher $E_{\rm B}$ with increasing θ and reaches $E_{\rm B}$ maximum around θ = 37°. It is noticed that a finite spin polarization of 30 % found above $E_{\rm F}$ is derived from spin polarized secondary electrons excited by both He I$_\beta$ ($h\nu$ = 23.1 eV) and He II$_\alpha$ ($h\nu$ = 40.8 eV) lines. Since the background intensities produced by He I$_\beta$ and He II$_\alpha$ are very poor, it should not influence on the following discussion throughout this paper should not be influenced.

Next, the experimentally determined energy dispersion curves are presented in Fig.3. It is found here that the experimental minority spin band A shows a downward energy dispersion along $\bar{\Gamma}-\bar{X}$ as shown with filled triangles, while the majority spin band B shows an upward dispersion as denoted by open triangles. The other weak emission features are also plotted with open square marks. It is recognized that the bottom of the energy dispersion curve of minority spin band (B) is located at $\bar{X}$ point in the surface Brillouin zone (SBZ). Here, the energy dispersions of A and B are compared with the calculation obtained by a tight-binding method along the thick curve shown in Fig.1 (c). In the calculation, only the first and second nearest neighbor atoms are considered. The transfer integrals such as ($sp\sigma$) and ($pd\sigma$) etc. have been determined by fitting to the reported pseudopotential calculation [15]. Here, the parameter of exchange splitting energy was set to 1.5 eV, which is the same as that reported by Fanelsa et al. [13]. Open (filled) circles represent the calculated band structure for majority (minority) spin states. The experimental energy dispersion curves are interpolated between the experimental data points for A and B. It is recognized that one of the calculated minority spin bands (α : filled circles) also shows the downward dispersion that reaches to the bottom at $\bar{X}$ point, which is similar to the experimental result for A. The observed band width and the dispersion feature are similar to the calculated one as shown in Fig.3. Besides, the experimental majority spin band B corresponds to the calculated band (β : open circles). Accordingly, these observed band structures (A and B) can be regarded as those

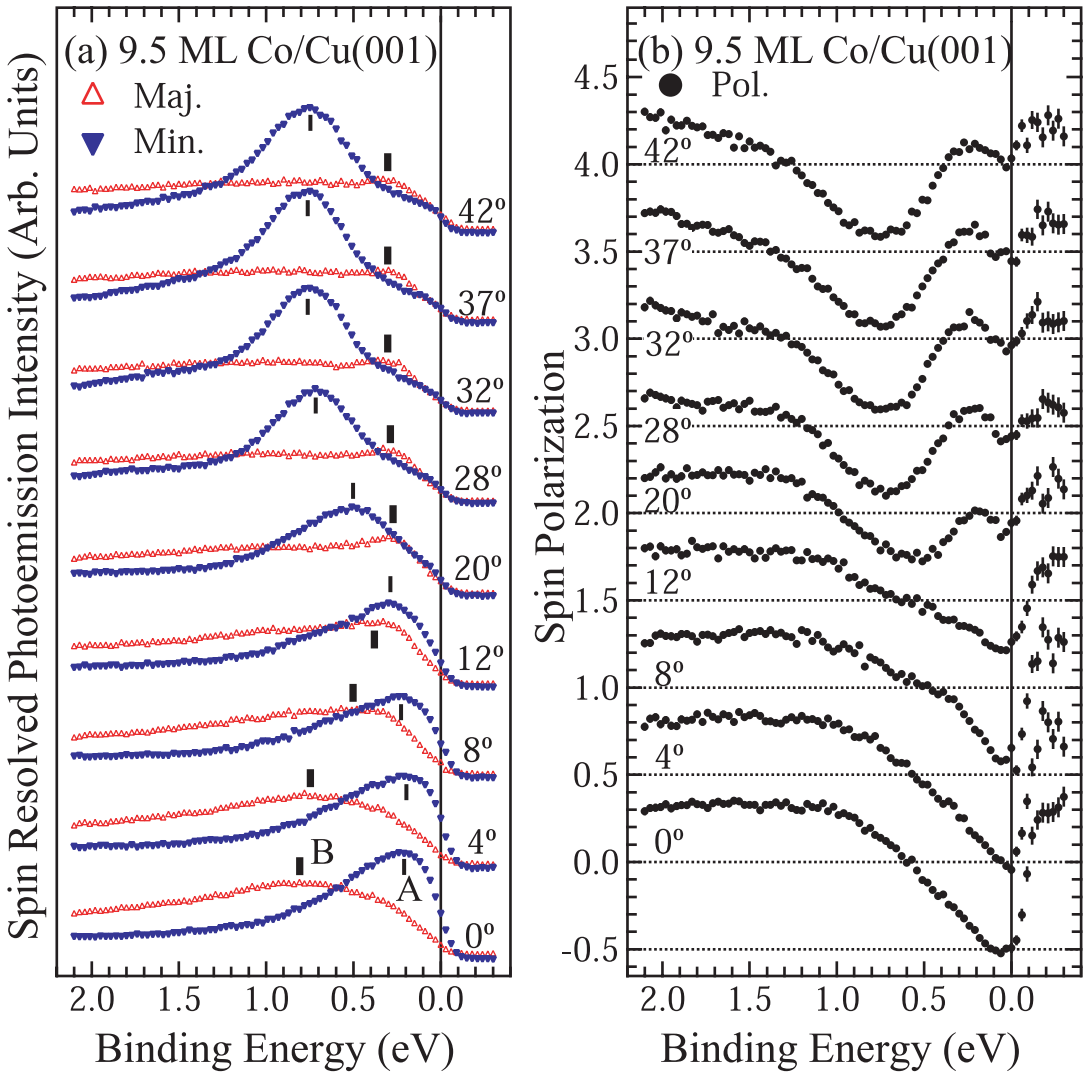

Figure 2. (a) SARPE spectra and (b) spin polarizations of 9.5 ML Co/Cu(001) with emission angles from 0° to 42°. Majority and minority spin spectra are shown with open and filled triangles, respectively. Thin (thick) vertical bars show the peak positions of Co 3*d* states in the minority (majority) spin channel. Origins of spin polarizations are shifted by 0.5 for every emission angle.

from bulk. At $\bar{\Gamma}$, minority and majority spin structures A and B can be assigned to $\Delta_{5\downarrow}$ and $\Delta_{2\uparrow}$ states, respectively. It is noted that only the states with Δ_1 and Δ_5 orbital symmetries can be accessible for the excitation with s- and p-polarized light. However, there is a possibility that the Δ_2 state can be observed due to an inter-band mixing of Δ_2 and Δ_5 bands through a spin-orbit coupling as shown in the similar argument for Cu(001) [16].

Figures 4 (a) - (d) show the observed SARPE spectra of the Co films with different thickness (2 - 9.5 ML) for majority and minority spin states at $\bar{\Gamma}$ and $\bar{X}$ points. Here, we mainly discuss the band structures A and B in the majority and minority spin channels. At first, in the majority spin state of Fig.4 (a), we find that the energy position of

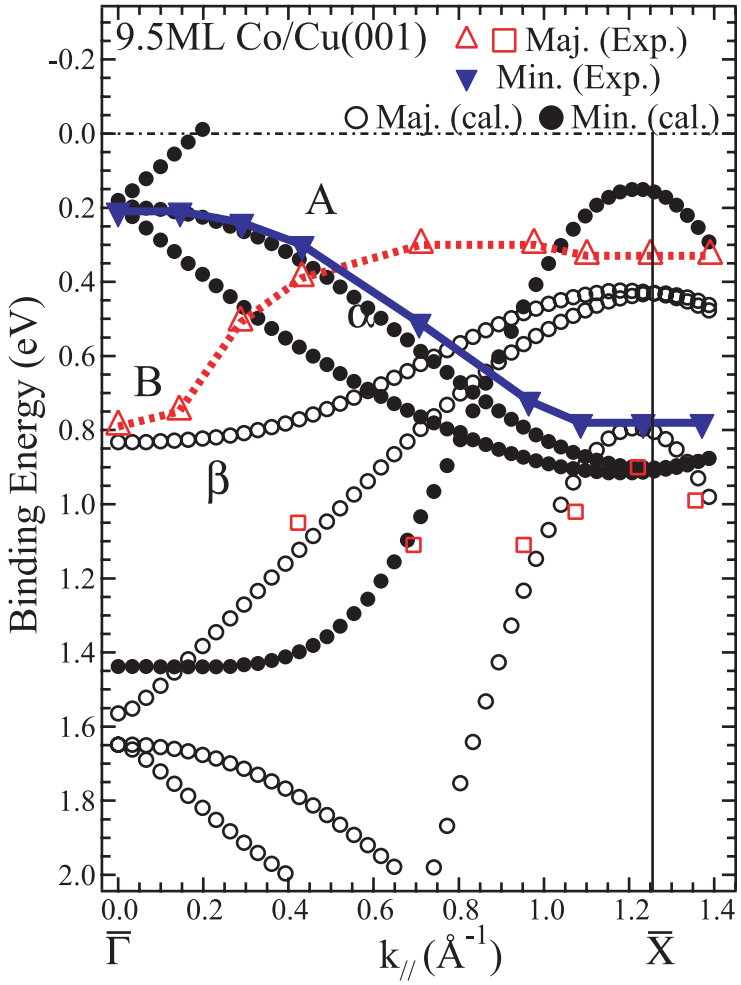

Figure 3. Experimental E_{B}-$k_{//}$ plots for majority and minority spin states as denoted by open and filled triangles, respectively. Solid and dashed lines show the interpolated band dispersions of bands A and B. Calculated bulk band structures obtained by tight-binding scheme are superposed with open and filled circles for majority and minority spin states, respectively.

structure B shifts toward higher E_B with increasing film thickness at $\bar{\Gamma}$ point. The energy difference of the spectra for 2 ML and 9.5 ML is about 400 meV. In the minority spin channel of Fig.4 (b) at $\bar{\Gamma}$ point, the peak A is located at lower E_B for thicker film and the maximum energy difference is as large as about 100 meV. In contrast, at $\bar{X}$ point, the energy position for the peak B (A) in majority (minority) spin channel shifts toward lower (higher) E_B with increasing film thickness. The largest energy shift of band B (A) is about 60 meV (270 meV). Thus, the observed energy shifts are dependent on the electronic states (A or B) as well as on the symmentry point of SBZ.

Figures 5 (a) and (b) are shown to clarify these experimental band dispersion curves of films with different thicknesses (2 - 9.5 ML) for the majority and minority spin states. As described in previous paragraph, the energy position of A shifts toward lower E_B with increasing film thickness at $\bar{\Gamma}$ point, while the behavior is opposite at $\bar{X}$ point.

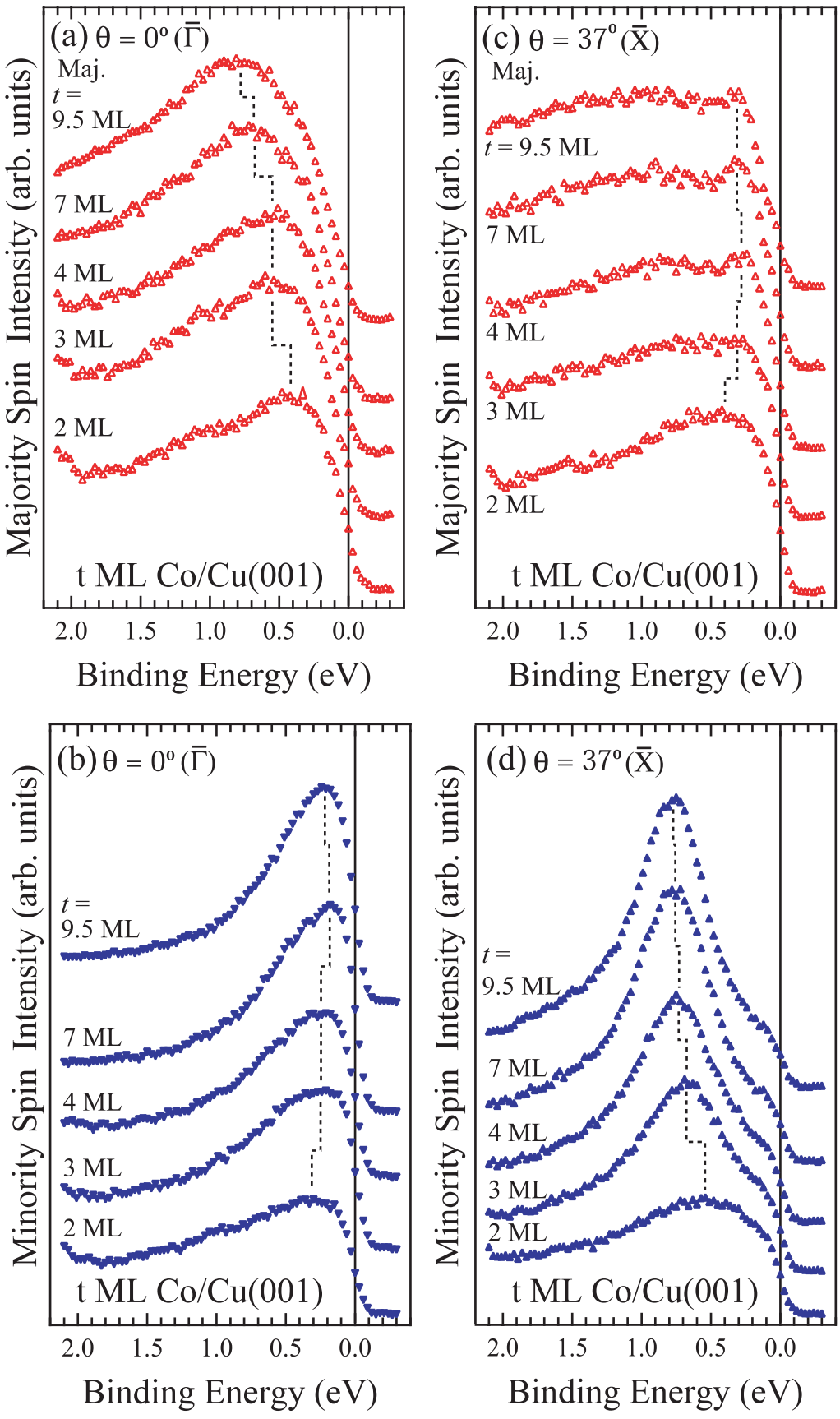

Figure 4. Majority (minority) spin spectra of t ML Co/Cu(001) with t = 2, 3, 4, 7 and 9.5 ML for $\theta = 0°$ [(a), (b)] and for $\theta = 37°$ [(c), (d)], corresponding to $\bar{\Gamma}$ and $\bar{X}$ points of surface Brillouin zone, respectively.

As a result, the band-width defined as the difference of peak positions between $\bar{\Gamma}$ and $\bar{X}$ of A appears to be narrower from 570 meV to 210 meV with decreasing the film thickness from 9.5 ML to 2 ML. As for the majority spin band B, the width is also narrowed from 460 meV to 60 meV when the film thickness decreases as shown in Fig.4 (a). In particular, the majority spin band B of 2 ML Co film seems to have negligible dispersion, while the minority spin band A for 2 ML Co film still appears to retain its dispersion. The thicker films above 7ML show the similar band-width for A, while for B, the width is still reduced by 100 meV. As reported in the previous paper by Schneider et al., the electronic structure of 5 ML fct-cobalt film is considered to be already bulk-like [12]. This is supported by the present result for the band A corresponding to the same symmetry (Δ_5 at $\bar{\Gamma}$). On the other hand, for the band B with different symmetry (Δ_2 at $\bar{\Gamma}$), the width is even different between 7ML and 9.5ML. The result means that the band structures with different spatial symmetry are affected by the film thickness in a different way. Moreover, the size of peak shift related to film thickness depends on the position of $k_{//}$ such as $\bar{\Gamma}$ and $\bar{X}$ as shown in Fig.4. According to the present analysis with tight-binding calculation, the band A is composed of only d_{xz} (d_{yz}) orbital at $\bar{\Gamma}$ and a linear combination of $d_{x^2-y^2}$ ($\sim$ 62 %), d_{xz} ($\sim$ 18 %) and d_{yz} ($\sim$ 18 %) at $\bar{X}$, where x-, y- and z-axes are defined along [100],[010] and [001] of Fig.1 (b). Similary, for the band B, it is only derived from $d_{x^2-y^2}$ orbital at $\bar{\Gamma}$ and composed of a linear combination of $d_{x^2-y^2}$ ($\sim$ 37 %), d_{xz} ($\sim$ 31 %), d_{yz} ($\sim$ 31 %) orbitals at $\bar{X}$. It is noted that the distinct energy shift emerges for the specific states dominated with $d_{x^2-y^2}$ orbital. It is considered that the narrower band width with decreasing film thickness indicates less delocalized feature of Co 3d electrons. If the electron localization is derived from a low dimensionality, the band-width would be narrow especialy along the normal direction to surface plane. Since the emission angle is varied with fixed photon energy in the present experiment, the band structures are traced not only along $k_{//}$ but also along $k_{\perp}$. One would expect the band narrowing along $k_{\perp}$ direction because the electron motion could be limited to the plane. However, this interpretation is incompatible with the observed narrowing of $d_{x^2-y^2}$ band that is spread along the surface plane. Here, the transfer integrals for the tight binding calculation which are sensitively dependent on the Co-Co distance, are responsible for the band width. Generally, the band width is narrower since the transfer integral becomes smaller when the Co-Co distance increases. Therefore, it is suggested that the Co-Co distance of the thin film is more expanded along in-plane direction for thinner film thickness, because the atomic distance of Cu is generally larger than that of Co [17, 18]. Besides, it is also needed to consider atomic inter-diffusion effect at the interface between Co and Cu layers instead of the electron localization due to a lower dimensionality. Actually, it is known that the in-plane lattice constant could be expanded as caused by atomic inter-diffusion because the surface energy of fcc Cu(001) is about a half as small as that of fcc Co(001) [19, 20]. Therefore, it is concluded that the observed feature of the band structure for thinner film thickness is mainly derived from the expanded lattice constant of Co film caused by the inter-diffusion effect or by the Cu substrate itself.

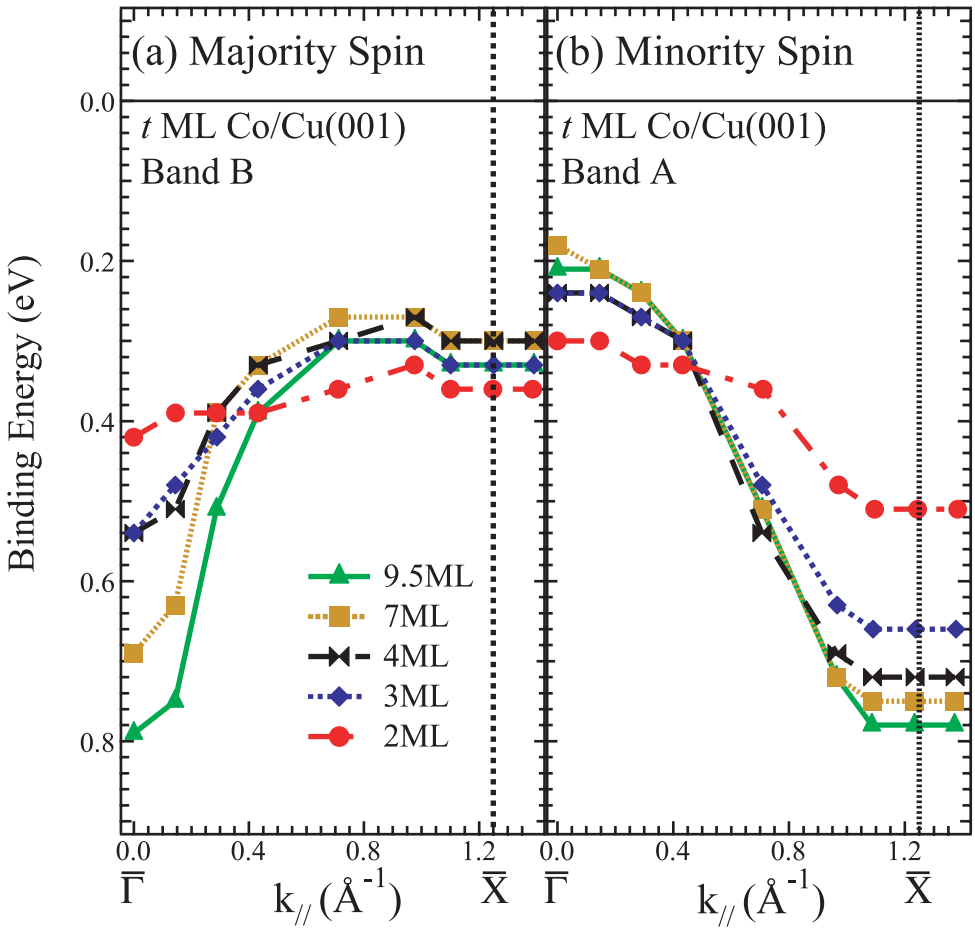

Figure 5. (a), (b) Experimental band dispersion curves for t ML Co/Cu(001) with t = 2, 3, 4, 7 and 9.5 ML for the bands B (left) and A (right).

4. Conclusion

In conclusion, we have done the spin- and angle- resolved photoemission spectroscopy to investigate variation of the spin-polarized electronic states for fct Co with changing the film thickness. It has been found that the majority and minority spin band dispersions becomes flatter as the Co film thickness decreases, indicating less hopping probability of the Co 3d electrons in the thinner film, which is not caused simply by the lower dimensionality but seriously by the increase of lateral lattice constant.

References

[1] W. L. O'Brien, T. Droubay and B. P. Tonner, Phys. Rev. B **54**, 9297 (1996).
[2] D. Matsumura, T. Yokoyama, K. Amamiya, S. Kitagawa and T. Ohta, Phys. Rev. B **66**, 024402 (2002).
[3] P. Gambardella, A. Dallmeyer, K. Maiti, M. C. Malagoli, W. Eberhardt, K. Kern, C. Carbone, Nature **416**, 301 (2002).

[4] C. M. Schneider, P. Schuster, M. Hammond, H. Ebert, J. Noffke and J. Kirschner, J. Phys. Condens. Matter **3**, 4349 (1991).
[5] F. Huang, M. T. Kief, G. J. Mankey, and R. F. Willis, Phys. Rev. B. **49**, 3962 (1994).
[6] M. Tischer, O. Hjortstam, D. Arvanitis, J. Hunter Dunn, F. May, K. Baberschke, J. Trygg, J. M. Wills, B. Johansson, and O. Eriksson, Phys. Rev. Lett. **75**, 1602 (1995).
[7] W. Clemens, E. Vescovo, T. Kachel, C. Carbone and W. Eberhardt, Phys. Rev. B **46**, 4198 (1992). / W. Clemens, T. Kachel, O. Rader, E. Vescovo, S. Bl*ü*gel, C. Carbone and W. Eberhardt, Solid state commun. **81**, 739 (1992).
[8] S. S. P. Parkin, R. Bhadra and K. P. Roche, Phys. Rev. Lett. 66, 2152 (1991).
[9] M. N. Baibich, J. M. Broto, A. Fert, F. Nguyen Van Dau, F. Petroff, P. Eitenne, G. Creuzet, A. Friederich, and J. Chazelas, Phys. Rev. Lett. **61**, 2472 (1988).
[10] S. Qiao, A. Kimura, A. Harasawa, M. Sawada, J. G. Chung, A. Kakizaki, Rev. Sci. Instrum. **68**, 4390 (1997).
[11] K. Iori, K. Miyamoto, H. Narita, K. Sakamoto, A. Kimura, S. Qiao, K. Shimada, H. Namatame, M. Taniguchi, Rev. Sci. Instrum. **77**, 013101 (2006).
[12] C. M. Schneider, J. J. de Miguel, P. Bressler, P. Schuster, R. Miranda and J. Kirschner, J. Electron Spectrosc. Relat. Phenom. **51**, 263 (1990).
[13] A. Fanelsa, E. Kisker, J. Henk and R. Feder, Phys. Rev. B **54**, 2922 (1996).
[14] J. Henk, T. Scheunemann, S. V. Halilov and R. Feder, J. Phys.: Condens. Matter **8**, 47 (1996).
[15] F. J. Himpsel, J. E. Ortega, G. M Mankey and R. F. Willis, Adv. Phys. **47**, 511 (1998).
[16] W. Kuch, M.-T. Lin, K. Meinel, and C. M. Schneider, J. Noffke, J. Kirschner **51**, 12627 (1995).
[17] C. Li, A. J. Freeman and C. L. Fu, J. Magn. Magn. Mat. **75**, 53 (1988).
[18] H. L. Luo and P. Duwez, Can. J. Phys. **41**, 758 (1963).
[19] J. Fassbender, R. Allenspach, U. D*ü*rig, Surf. Sci. **383**, L742 (1997).
[20] P. Poulopoulos, P. J. Jensen, A. Ney, J. Lindner and K. Baberschke, **65**, 064431 (2002).